Electrical Power and Energy Systems 56 (2014) 228–234

Contents lists available at ScienceDirect

Electrical Power and Energy Systems

journal homepage: www.elsevier.com/locate/ijepes

Modeling of three-phase autotransformer for short-circuit studies

Dalibor Filipović-Grčić [a], Božidar Filipović-Grčić [b,*], Kosjenka Capuder [c]

[a] Končar Electrical Engineering Institute, Fallerovo šetalište 22, 10000 Zagreb, Croatia
[b] University of Zagreb, Faculty of Electrical Engineering and Computing, Unska 3, 10000 Zagreb, Croatia
[c] Končar Power Transformers, Josipa Mokrovića 6, 10090 Zagreb, Croatia

ARTICLE INFO

Article history:
Received 11 August 2013
Received in revised form 28 October 2013
Accepted 6 November 2013

Keywords:
Autotransformer
Inductance matrix model
Short-circuit
Symmetrical components
Tertiary winding

ABSTRACT

In this paper a three-phase autotransformer is represented by inductance matrix for short-circuit studies. The inductance matrix consists of winding self-inductances and corresponding mutual inductances between windings. For single phase-to-ground fault the inductance matrix model results are compared to symmetrical components results, commonly used to analyze unsymmetrical faults in three-phase power systems. The influence of a delta connected tertiary winding on un-faulted phase voltages and asymmetrical fault current distribution is analyzed.

1. Introduction

The autotransformer is a power transformer in which one winding, known as the common or parallel winding, is shared between the high voltage (HV) and the low voltage (LV) circuit. As a part of the power transmission system, in service the autotransformer is exposed to various voltage and current stresses. Short-circuit currents cause thermal and mechanical stresses of transformer windings, while the ground fault occurrence in network with an isolated neutral point may result in un-faulted phase voltages significantly higher than operating voltages [1]. As a consequence, an internal winding fault can occur and eventually lead to insulation failure [2,3].

The autotransformer zero sequence impedance highly depends on delta winding presence. For this reason, delta winding is commonly used to provide a low impedance path for third harmonic currents and to reduce current and voltage imbalances caused by asymmetrical loading, but also for other purposes such as to connect compensation. Delta connected tertiary winding is usually sized for at least one third of the rated power and having the lowest rated voltage. The tertiary must withstand the effects of a short-circuit fault across its external terminals, as well as those due to earth faults on the main windings. An embedded delta tertiary winding, sometimes referred to as a stabilization winding, improves the availability of the transformer by eliminating the occurrence of tertiary lead faults since only two connections from the phases, forming one corner of the delta that is grounded, are brought out of the transformer.

In Ref. [4] three winding transformer model for short-circuit studies is presented. The model takes into account off-nominal tap positions and the phase shifts among the windings.

A systematic approach to solving power system faults using the three terminal Thevenin's equivalent circuit is presented in [5] and demonstrated in case of symmetrical and unsymmetrical faults.

Papers [6,7] describe the autotransformer models for load-flow, short-circuit [8] and transient recovery voltage analysis [9]. High-frequency autotransformer model derived from the results of a lightning electromagnetic pulse test is presented in [10]. Ref. [11] describes the influence of a delta connected tertiary winding on voltages and currents during fault conditions.

The contribution of this paper is the development of autotransformer inductance matrix model for short-circuit studies. Model was developed and verified in Matlab/M-file [12]. The application of this model could be useful when performing short-circuit system studies needed for autotransformer dimensioning and protection relay setting [13,14]. The influence of a delta connected tertiary winding on un-faulted phase voltages and fault currents was analyzed.

2. Three-phase autotransformer model based on inductance matrix

In autotransformer the HV circuit is composed of the common winding and the series winding while the LV circuit is composed only of the common winding [15].

* Corresponding author. Tel.: +385 1 6129 714; fax: +385 1 6129 890.
E-mail addresses: dfilipovic@koncar-institut.hr (D. Filipović-Grčić), bozidar.filipovic-grcic@fer.hr (B. Filipović-Grčić), kosjenka.capuder@siemens.com (K. Capuder).

0142-0615/$ - see front matter © 2013 Elsevier Ltd. All rights reserved.
http://dx.doi.org/10.1016/j.ijepes.2013.11.005

The proposed autotransformer model consists of winding self-inductances and corresponding mutual inductances between windings. In power transformers the resistance component of the impedance is negligible in comparison with the inductance component, thus only the inductive component is considered in the following calculations. This approximation slightly overestimates short-circuits currents.

All model parameters can be obtained from factory measurements and manufacturer data. First, the total self-inductance L_1 of series and parallel winding is determined from open-circuit test data (1):

$$L_1 = \frac{U_{r1}^2}{\omega \cdot I_0 \cdot S_r} \cdot 100, \tag{1}$$

where I_0 is the magnetizing current in percent of the rated current, U_{r1} is the rated voltage of HV winding, S_r is the rated power and ω is the angular frequency.

Afterwards, the self-inductances L_S of the series winding, L_P of the parallel winding and L_3 of the tertiary winding are determined from the following expressions:

$$L_S = L_1 \cdot \left(\frac{U_{r1} - U_{r2}}{U_{r1}}\right)^2, \tag{2}$$

$$L_P = L_1 \cdot \left(\frac{U_{r2}}{U_{r1}}\right)^2, \tag{3}$$

$$L_3 = \frac{U_{r3}^2}{\omega \cdot I_0 \cdot S_{r1}} \cdot 100 \cdot 3, \tag{4}$$

where U_{r2} is the rated voltage of the parallel winding and U_{r3} is the rated voltage of tertiary winding.

Mutual inductance M_{SP}between series and parallel winding can be determined from the test circuit shown in Fig. 1. LV winding is short-circuited and voltage is increased on HV side until rated current I_{r1} is reached.

The phase angle of the applied voltage is assumed to be 0° and current I_{r1} lags by 90° since the load is purely inductive. Value of the current through parallel winding I_2 is unknown but the direction is opposite to I_{r1}. The Eqs. (5) and (6) are derived from the test circuit shown in Fig. 1.

$$\frac{U_{r1}}{\sqrt{3}} \cdot \frac{u_{kr12}}{100} = I_{r1}\omega(L_S + M_{SP}) - I_2\omega(L_P + M_{SP}) \tag{5}$$

$$I_2 = I_{r1}\frac{M_{SP}}{L_P} \tag{6}$$

u_{kr12} is the rated short-circuit voltage of a transformer referred to rated apparent power S_{r12} between HV and LV winding. U_{r1} is the rated voltage of HV winding. M_{SP} is determined by substituting I_2 in (5) with expression (6).

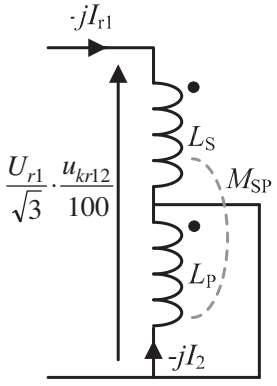

Fig. 1. Test circuit used for determination of M_{SP}.

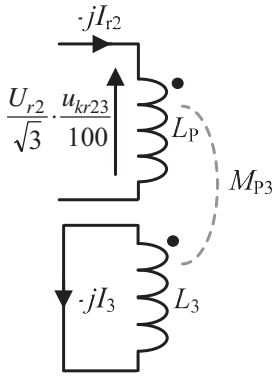

Fig. 2. Test circuit used for determination of M_{P3}.

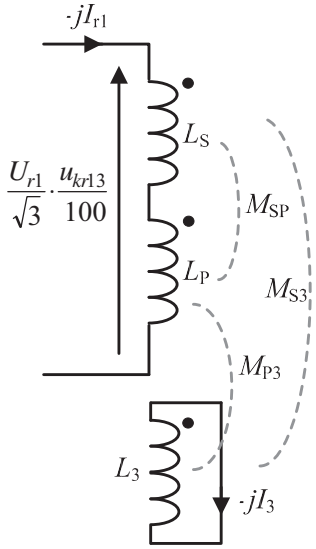

Fig. 3. Test circuit used for determination of M_{S3}.

$$M_{SP} = \sqrt{\left(I_{r1}\omega L_S - \frac{U_{r1}}{\sqrt{3}} \cdot \frac{u_{kr12}}{100}\right) \cdot \frac{L_P}{\omega I_{r1}}} \tag{7}$$

Mutual inductance M_{P3} between parallel and tertiary winding can be determined from the test circuit shown in Fig. 2. Voltage is applied on LV winding, while the tertiary winding is short-circuited.

The Eqs. (8) and (9) are derived from the test circuit shown in Fig. 2.

$$\frac{U_{r2}}{\sqrt{3}} \cdot \frac{u_{kr23}}{100} = I_{r2}\omega L_P - I_3\omega M_{P3} \tag{8}$$

$$I_3 = I_{r2}\frac{M_{P3}}{L_3} \tag{9}$$

u_{kr23} is the rated short-circuit voltage of a transformer referred to rated apparent power S_{r23} between LV and tertiary winding. U_{r2} is the rated voltage of LV winding. From Eqs. (8) and (9) M_{P3} is determined (10).

$$M_{P3} = \sqrt{\left(I_{r2}\omega L_P - \frac{U_{r2}}{\sqrt{3}} \cdot \frac{u_{kr23}}{100}\right) \cdot \frac{L_3}{\omega I_{r2}}} \tag{10}$$

Mutual inductance M_{S3} between series and tertiary winding can be determined from the test circuit shown in Fig. 3 and from the results of previous tests. Voltage is applied on HV side, while the tertiary winding is short-circuited.

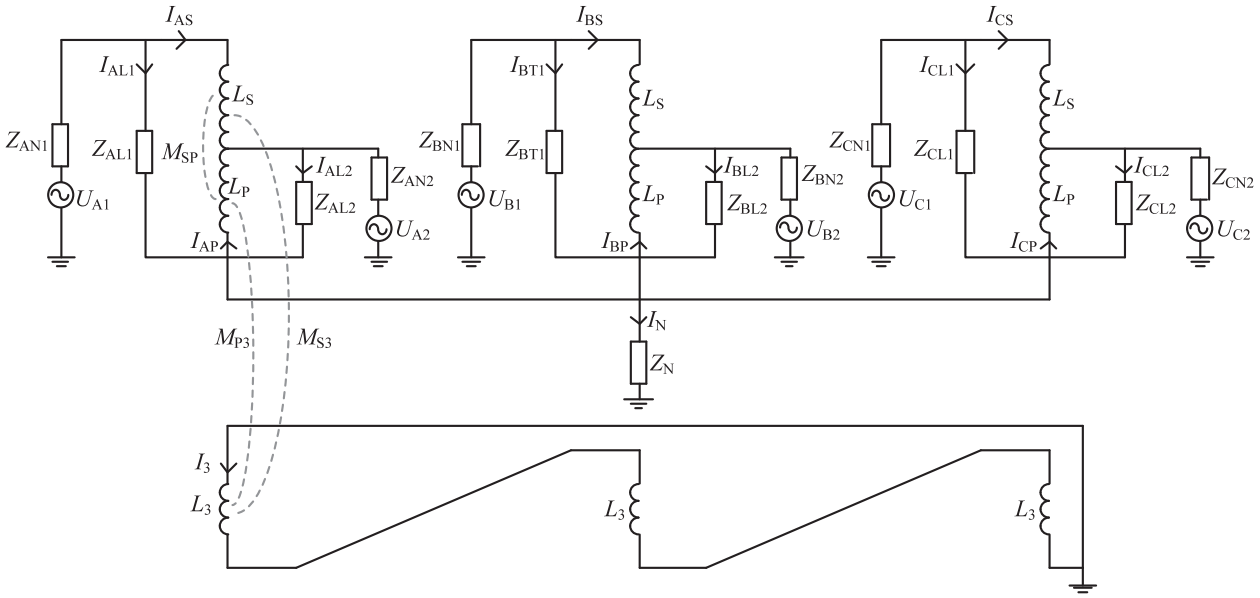

Fig. 4. Autotransformer three-phase representation for short-circuit studies.

The Eqs. (11) and (12) are derived from the test circuit shown in Fig. 3.

$$\frac{U_{r1}}{\sqrt{3}} \cdot \frac{u_{kr13}}{100} = I_{r1}\omega(L_S + L_P + 2M_{SP}) - I_3\omega(M_{S3} + M_{P3}) \tag{11}$$

$$I_3 = I_{r1}\frac{M_{S3} + M_{P3}}{L_3} \tag{12}$$

u_{kr13} is the rated short-circuit voltage of a transformer referred to rated apparent power S_{r13} between HV and tertiary winding. By including Eq. (12) into (11) M_{S3} is determined (13).

$$M_{S3} = \sqrt{L_3 \cdot (L_S + L_P + 2M_{SP}) - \frac{U_{r1}}{\sqrt{3}} \cdot \frac{u_{kr13}}{100} \cdot \frac{L_3}{\omega I_{r1}}} - M_{P3} \tag{13}$$

Active networks connected to HV and LV side are represented with voltage sources and impedances Z_{AN1} and Z_{AN2}:

$$Z_{AN1} = j\frac{U_{r1}^2}{S_{sc1}} \tag{14}$$

$$Z_{AN2} = j\frac{U_{r2}^2}{S_{sc2}} \tag{15}$$

where S_{sc1} and S_{sc2} are short-circuit powers of active networks on HV and LV side, respectively. The autotransformer model is presented in Fig. 4.

Impedances Z_{AL1} and Z_{AL2} from Fig. 4 are used to simulate short-circuits on HV and LV side, while Z_N represents the impedance of the autotransformer ground impedance.

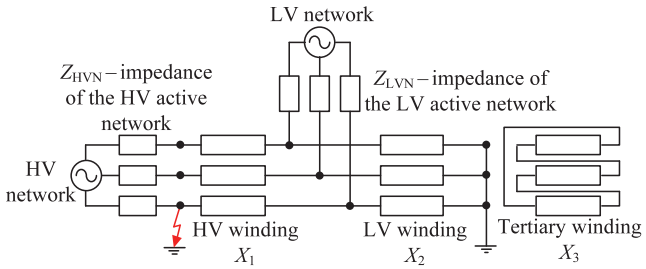

Fig. 5. Equivalent scheme of single phase-to-ground fault on HV side of three-phase autotransformer.

Kirchhoff's voltage law equations for HV side phase A are given in (16) and (17).

$$U_{A1} = (I_{AL1} + I_{AS}) \cdot Z_{AN1} + I_{AS}j\omega L_S - I_{AP}j\omega L_P + I_N Z_N - I_{AP}j\omega M_{SP} + I_{AS}j\omega M_{SP} + I_3 j\omega M_{S3} + I_3 j\omega M_{P3} \tag{16}$$

$$U_{A1} = (I_{AL1} + I_{AS}) \cdot Z_{AN1} + I_{AL1}Z_{AL1} + I_N Z_N \tag{17}$$

Analogous to (16) and (17) the equations are derived for phases B and C at HV. Kirchhoff's voltage law equations for LV side phase A are given in (18) and (19).

$$U_{A2} = (I_{AL2} - I_{AS} - I_{AP}) \cdot Z_{AN2} - I_{AP}j\omega L_P + I_N Z_N + I_{AS}j\omega M_{SP} + I_3 j\omega M_{P3} \tag{18}$$

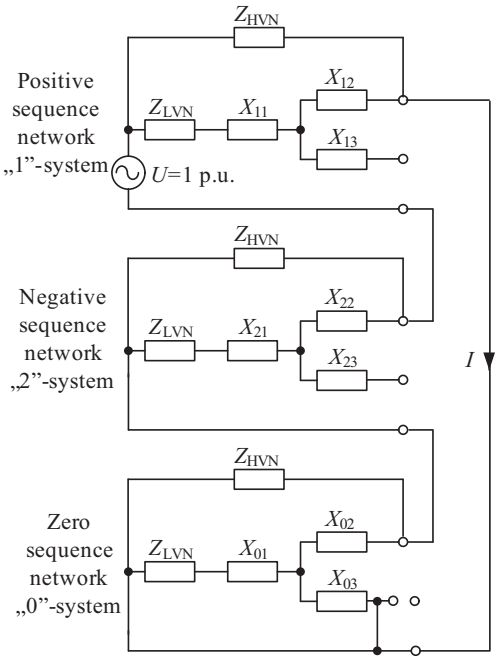

Fig. 6. Single phase-to-ground fault on HV side modeled using symmetrical components.

$$U_{A2} = (I_{AL2} - I_{AS} - I_{AP}) \cdot Z_{AN2} + I_{AL2}Z_{AL2} + I_N Z_N \quad (19)$$

Analogous to (18) and (19) the equations are derived for phases B and C at LV side.

Two more equations are derived from Kirchhoff's current law:

$$(I_{AP} + I_{BP} + I_{CP}) \cdot j\omega M_{P3} = (I_{AS} + I_{BS} + I_{CS}) \cdot j\omega M_{S3} + 3I_3 \cdot j\omega L_3 \quad (20)$$

$$I_{AP} + I_{BP} + I_{CP} + I_N = I_{AL1} + I_{BL1} + I_{CL1} + I_{AL2} + I_{BL2} + I_{CL2} \quad (21)$$

The per unit short-circuit impedances are calculated by Eqs. (29)–(31).

$$X_{HV/LV} = \frac{u_{kr12}}{100} \quad (29)$$

$$X_{HV/TV} = \frac{u_{kr13}}{100} \quad (30)$$

$$X_{LV/TV} = \frac{u_{kr23}}{100} \quad (31)$$

$$\begin{bmatrix} U_{A1} \\ U_{B1} \\ U_{C1} \\ U_{A2} \\ U_{B2} \\ U_{C2} \\ U_{A1} \\ U_{B1} \\ U_{C1} \\ U_{A2} \\ U_{B2} \\ U_{C2} \\ 0 \\ 0 \end{bmatrix} = \begin{bmatrix} Z_{AN1} & 0 & 0 & 0 & 0 & 0 & Z_{AN1}+X_S+X_{SP} & 0 & 0 & -(X_P+X_{SP}) & 0 & 0 & Z_N & X_{S3}+X_{P3} \\ 0 & Z_{BN1} & 0 & 0 & 0 & 0 & 0 & Z_{BN1}+X_S+X_{SP} & 0 & 0 & -(X_P+X_{SP}) & 0 & Z_N & X_{S3}+X_{P3} \\ 0 & 0 & Z_{CN1} & 0 & 0 & 0 & 0 & 0 & Z_{CN1}+X_S+X_{SP} & 0 & 0 & -(X_P+X_{SP}) & Z_N & X_{S3}+X_{P3} \\ 0 & 0 & 0 & Z_{AN2} & 0 & 0 & X_{SP}-Z_{AN2} & 0 & 0 & -(Z_{AN2}+X_P) & 0 & 0 & Z_N & X_{P3} \\ 0 & 0 & 0 & 0 & Z_{BN2} & 0 & 0 & X_{SP}-Z_{BN2} & 0 & 0 & -(Z_{BN2}+X_P) & 0 & Z_N & X_{P3} \\ 0 & 0 & 0 & 0 & 0 & Z_{CN2} & 0 & 0 & X_{SP}-Z_{CN2} & 0 & 0 & -(Z_{CN2}+X_P) & Z_N & X_{P3} \\ Z_{AN1}+Z_{AL1} & 0 & 0 & 0 & 0 & 0 & Z_{AN1} & 0 & 0 & 0 & 0 & 0 & Z_N & 0 \\ 0 & Z_{BN1}+Z_{BL1} & 0 & 0 & 0 & 0 & 0 & Z_{BN1} & 0 & 0 & 0 & 0 & Z_N & 0 \\ 0 & 0 & Z_{CN1}+Z_{CL1} & 0 & 0 & 0 & 0 & 0 & Z_{CN1} & 0 & 0 & 0 & Z_N & 0 \\ 0 & 0 & 0 & Z_{AN2}+Z_{AL2} & 0 & 0 & -Z_{AN2} & 0 & 0 & -Z_{AN2} & 0 & 0 & Z_N & 0 \\ 0 & 0 & 0 & 0 & Z_{BN2}+Z_{BL2} & 0 & 0 & -Z_{BN2} & 0 & 0 & -Z_{BN2} & 0 & Z_N & 0 \\ 0 & 0 & 0 & 0 & 0 & Z_{CN2}+Z_{CL2} & 0 & 0 & -Z_{CN2} & 0 & 0 & -Z_{CN2} & Z_N & 0 \\ 0 & 0 & 0 & 0 & 0 & 0 & X_{S3} & X_{S3} & X_{S3} & -X_{P3} & -X_{P3} & -X_{P3} & 0 & 3X_3 \\ -1 & -1 & -1 & -1 & -1 & -1 & 0 & 0 & 0 & 1 & 1 & 1 & 1 & 0 \end{bmatrix} \times \begin{bmatrix} I_{AL1} \\ I_{BL1} \\ I_{CL1} \\ I_{AL2} \\ I_{BL2} \\ I_{CL2} \\ I_{AS} \\ I_{BS} \\ I_{CS} \\ I_{AP} \\ I_{BP} \\ I_{CP} \\ I_N \\ I_3 \end{bmatrix} \quad (22)$$

Kirchhoff's law equations can be written in matrix form (22) which can be simplified as:

$$[I] = [Z]^{-1} \times [U] \quad (23)$$

The unknown current vector [**I**] is calculated as a product of the inverted matrix [**Z**] and the vector [**U**] with known nodal voltages.

3. Symmetrical components model for single phase-to-ground fault

The autotransformer model for short-circuit studies was verified with symmetrical components [16]. Symmetrical components are commonly used to analyze unsymmetrical faults in three-phase power systems since in many cases the unbalanced part of the physical system can be isolated for a study, while the rest of the system is being considered to be in balance. In such cases, the aim is to find the symmetrical components of the voltages and the currents at the point of unbalance and connect the sequence networks.

Fig. 5 shows equivalent scheme for the analysis of single phase-to-ground fault on HV side of three-phase autotransformer.

Per unit impedances of active networks can be calculated by Eqs. (24) and (25).

$$Z_{HVN} = \frac{S_b}{S_{scHV}} \quad (24)$$

$$Z_{LVN} = \frac{S_b}{S_{scLV}} \quad (25)$$

S_b is base power and S_{scHV} and S_{scLV} are short-circuit powers of active networks.

Currents relevant to the base power are given by Eqs. (26)–(28).

$$I_{r1} = \frac{S_b}{\sqrt{3} \cdot U_{r1}} \quad (26)$$

$$I_{r2} = \frac{S_b}{\sqrt{3} \cdot U_{r2}} \quad (27)$$

$$I_{r3} = \frac{S_b}{3 \cdot U_{r3}} \quad (28)$$

Short-circuit reactances of the primary X_1, secondary X_2 and tertiary winding X_3, referring to Fig. 5, can be calculated by Eqs. (32)–(34).

$$X_1 = \frac{1}{2} \cdot (X_{HV/LV} + X_{HV/TV} - X_{LV/TV}) \quad (32)$$

$$X_2 = \frac{1}{2} \cdot (X_{HV/LV} + X_{LV/TV} - X_{HV/TV}) \quad (33)$$

$$X_3 = \frac{1}{2} \cdot (X_{HV/TV} + X_{LV/TV} - X_{HV/LV}) \quad (34)$$

Reactances of the transformer windings in positive (X_{11},X_{12},X_{13}), negative (X_{21},X_{22},X_{23}) and zero (X_{01},X_{02},X_{03}) sequence systems are determined by the Eqs. (35)–(37).

$$X_{11} = X_{21} = X_{01} = X_1 \quad (35)$$

$$X_{12} = X_{22} = X_{02} = X_2 \quad (36)$$

$$X_{13} = X_{23} = X_{03} = X_3 \quad (37)$$

Equivalent scheme of single phase-to-ground fault on HV side modeled using symmetrical components is shown in Fig. 6.

Total impedances of the positive, negative and zero sequence networks are determined using the Eqs. (38)–(41).

$$Z_1 = \frac{Z_{1HVN} \cdot (Z_{1LVN} + X_{11} + X_{12})}{Z_{1LVN} + Z_{1HVN} + X_{11} + X_{12}} \quad (38)$$

$$Z_2 = \frac{Z_{2HVN} \cdot (Z_{2LVN} + X_{21} + X_{22})}{Z_{2LVN} + Z_{2HVN} + X_{21} + X_{22}} \quad (39)$$

$$Z_p = \frac{X_{03} \cdot (Z_{0LVN} + X_{02})}{X_{03} + Z_{0LVN} + X_{02}} \quad (40)$$

$$Z_0 = \frac{Z_{0HVN} \cdot (Z_p + X_{01})}{Z_{0HVN} + Z_p + X_{01}} \quad (41)$$

Total currents of positive, negative and zero-sequence networks are determined by Eq. (42).

$$I_1 = I_2 = I_0 = I = \frac{U}{Z_1 + Z_2 + Z_0} \quad (42)$$

Positive-sequence currents of HV and LV side are determined by Eq. (43).

$$I_{11} = I_{12} = I \cdot \frac{Z_{1HVN}}{Z_{1LVN} + Z_{1HVN} + X_{11} + X_{12}} \tag{43}$$

Negative-sequence currents of HV and LV side are determined by Eq. (44).

$$I_{21} = I_{22} = I_{11} \tag{44}$$

Zero-sequence currents are determined by Eqs. (45)–(47).

$$I_{01} = I \cdot \frac{Z_{1HVN}}{Z_{0HVN} + Z_p + X_{01}} \tag{45}$$

$$I_{02} = I_{01} \cdot \frac{X_{03}}{Z_{0LVN} + X_{02} + X_{03}} \tag{46}$$

$$I_{03} = I_{01} - I_{02} \tag{47}$$

Finally, currents through HV, LV and tertiary winding are determined by Eqs. (48)–(50).

$$I_1 = (I_{11} + I_{21} + I_{01}) \cdot I_{r1} \tag{48}$$

$$I_2 = (I_{12} + I_{22} + I_{02}) \cdot I_{r2} - I_1 \tag{49}$$

$$I_3 = I_{03} \cdot I_r \tag{50}$$

4. Calculation examples

Calculations were performed on autotransformer with data given in Table 1.

Rated autotransformer powers are $S_{r1} = S_{r2} = 400$ MVA, $S_{r3} = 80$ MVA. Short-circuit powers of active networks are $S_{scLV} = 3.43$ GVA and $S_{scHV} = 11.9$ GVA.

4.1. Single phase-to-ground fault on HV side

Inductance matrix model was compared to symmetrical components for single phase-to-ground fault on HV side of three-phase autotransformer with solidly grounded neutral. Calculation results are shown in Table 2 and the percentage difference between fault currents is calculated. Calculation results with both autotransformer models show excellent agreement for different tap positions.

Table 1
Autotransformer data.

Tap	U_{r1} (kV)	U_{r2} (kV)	U_{r3} (kV)	u_{kr12}(%)	u_{kr13} (%)	u_{kr23} (%)
+	439.87	231	13.0	9.47	10.94	9.46
0	400	231	10.5	11.63	13.92	10.66
–	371.75	231	8.76	14.14	17.02	12.14

4.2. Influence of tertiary winding on un-faulted phase voltages for different grounding impedances

Autotransformer neutral is sometimes isolated in order to reduce the short circuit currents in power system. In case of ground fault in solidly grounded network the un-faulted phase voltages remain unchanged, but in isolated network un-faulted phase voltages will reach the phase-to-phase values. This would almost certainly result in over excitation of the core, with greatly increased magnetizing currents and core losses.

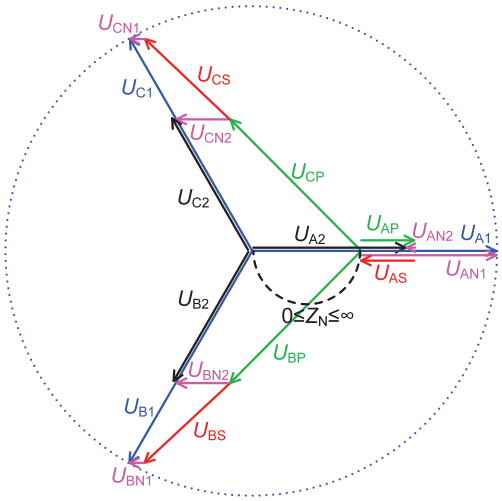

Fig. 7. Phasor diagram in case of isolated neutral $Z_N \to \infty$.

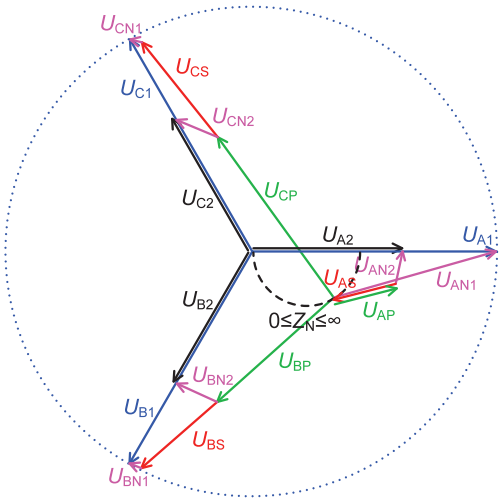

Fig. 8. Phasor diagram in case of neutral grounding impedance $Z_N = 10\ \Omega$.

Table 2
Calculation results.

Tap position	Current	Current values for inductance matrix model (A)	Current values for symmetrical components model (A)	Difference (ppm)
High tap	I_3	24308.1585	24308.1909	1.33
	I_{AS}	3406.4256	3406.4283	0.80
	I_{AP}	710.6559	710.6554	0.76
Principal tap	I_3	23137.1589	23137.2034	1.92
	I_{AS}	3194.4801	3194.4835	1.06
	I_{AP}	515.5074	515.5073	0.13
Low tap	I_3	22225.8374	22225.8968	2.67
	I_{AS}	2980.4587	2980.4629	1.39
	I_{AP}	356.1546	356.1552	1.68

Delta connected tertiary winding acts as short-circuit in zero sequence network and therefore reduces zero sequence impedance. As a consequence, the un-faulted phase voltages will be reduced.

The following example illustrates the effect of tertiary winding on un-faulted phase voltages for different grounding impedances. The single phase-to-ground fault was analyzed and the autotransformer was represented with inductance matrix.

Fig. 7 shows the voltage phasor diagram in case of isolated autotransformer neutral. Black dotted line indicates the half-circular path of neutral point potential with respect to ground impedance.

The results show that tertiary winding reduces overvoltages in un-faulted phases by 28.6% in case of isolated neutral. Fig. 8 shows the voltage phasor diagram when Z_N = 10 Ω, to illustrate the condition when neutral point is neither directly grounded nor isolated.

4.3. Influence of tertiary winding on asymmetrical fault current distribution

In case of an asymmetrical fault current flows through tertiary winding. The following examples, calculated with inductance matrix model, show the influence of tertiary winding presence on HV and LV side currents.

Figs. 9–12 show ampere-turns diagrams for asymmetrical faults on autotransformer with and without tertiary winding. Black dotted line represents translated ampere-turns phasor I_3N_3 which is equal to difference between parallel and serial winding ampere-turns. It can be seen that tertiary winding presence reduces the currents in un-faulted windings, but increases currents in faulty ones.

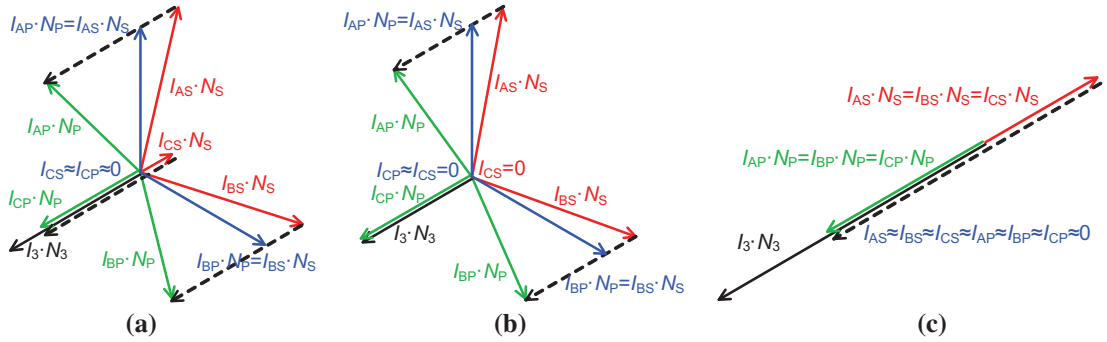

Fig. 9. Ampere-turns phasor diagrams for double phase-to-ground fault (phases A and B) on HV side supplied from: (a) HV and LV side; (b) LV side only; and (c) HV side only. Blue markings refer to case without tertiary winding. (For interpretation of the references to color in this figure legend, the reader is referred to the web version of this article.)

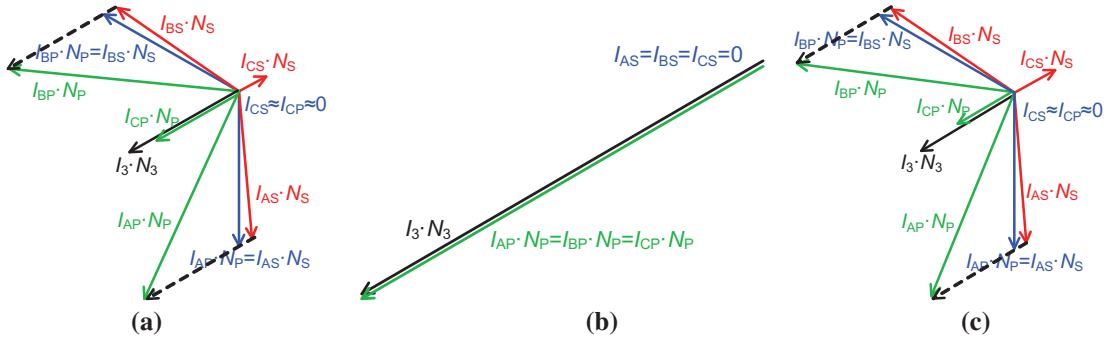

Fig. 10. Ampere-turns phasor diagrams for double phase-to-ground fault (phases A and B) on LV side supplied from: (a) HV and LV side; (b) LV side only; and (c) HV side only. Blue markings refer to case without tertiary winding. (For interpretation of the references to color in this figure legend, the reader is referred to the web version of this article.)

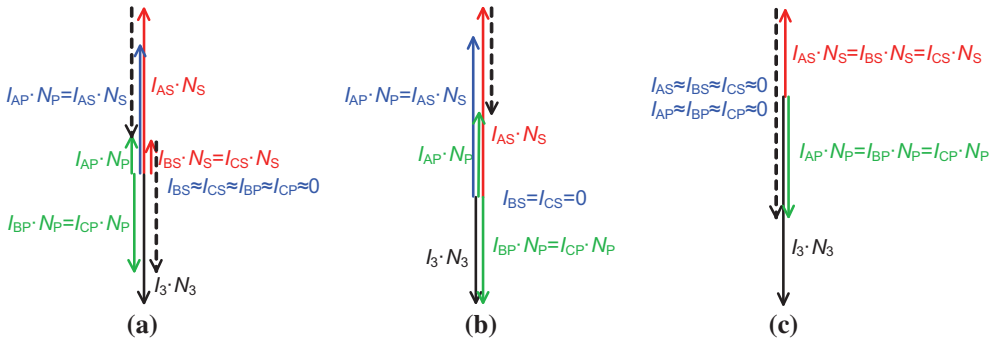

Fig. 11. Ampere-turns phasor diagrams for single phase-to-ground fault (phase A) on HV side supplied from: (a) HV and LV side; (b) LV side only; and (c) HV side only. Blue markings refer to case without tertiary winding. (For interpretation of the references to color in this figure legend, the reader is referred to the web version of this article.)

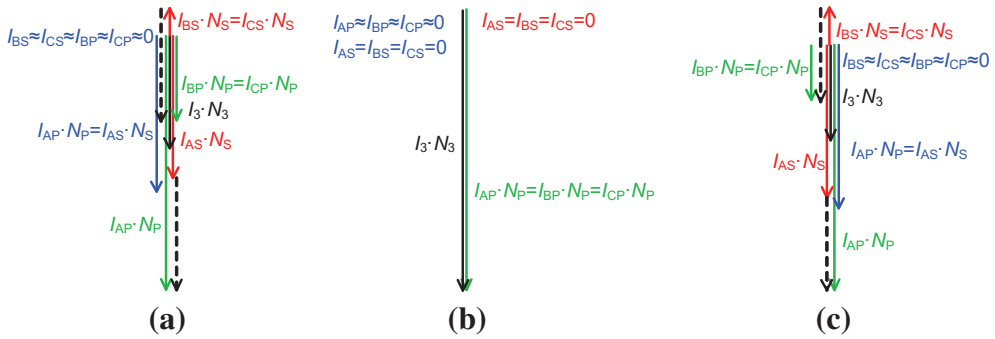

Fig. 12. Ampere-turns phasor diagrams for single phase-to-ground fault (phase A) on LV side supplied from: (a) HV and LV side; (b) LV side only; and (c) HV side only. Blue markings refer to case without tertiary winding. (For interpretation of the references to color in this figure legend, the reader is referred to the web version of this article.)

5. Conclusion

The inductance matrix autotransformer model for short-circuit studies is presented. The proposed model consists of winding self-inductances and corresponding mutual inductances between windings which are calculated from factory measurements and manufacturer data.

The model was verified with symmetrical components for single phase-to-ground fault and the results showed excellent agreement.

Additionally, the influence of tertiary winding on un-faulted phase voltages and on asymmetrical fault current distribution was analyzed. From the conducted analysis the following conclusions can be emphasized.

- The presence of tertiary winding significantly reduces temporary overvoltages in networks with isolated neutral. Neutral point potential moves along the half-circular path with respect to ground impedance.
- Asymmetrical fault currents in autotransformer HV and LV windings highly depend on delta winding presence. Tertiary winding presence increases currents in faulty windings, but reduces the currents in un-faulted ones.

  Some benefits of the inductance matrix model compared to symmetrical components model are:
- It is suitable for analyzing specific problems, i.e. the influence of tertiary winding on un-faulted phase voltages and fault current distribution, as described in chapter 4.
- It could be easily used in any standard transient simulation environment, including EMTP-like tools.
- It is possible to study easily different simultaneous faults on HV and LV side. Though relatively infrequent, simultaneous faults are important because relay systems, operating satisfactorily for single faults, may fail to isolate simultaneous faults. The analysis of simultaneous faults is considerably more complicated when using symmetrical components.

References

[1] Winders Jr JJ. Power transformers principles and applications. PPL electric utilities. Allentown, Pennsylvania: Marcel Dekker; 2002.
[2] Behjat V, Vahedi A, Setayeshmehr A, Borsi H, Gockenbach E. Sweep frequency response analysis for diagnosis of low level short circuit faults on the windings of power transformers: an experimental study. Int J Elect Power Energy Syst 2012;42(1):78–90.
[3] Rahmatian M, Vahidi B, Ghanizadeh AJ, Gharehpetian GB, Alehosseini HA. Insulation failure detection in transformer winding using cross-correlation technique with ANN and k-NN regression method during impulse test. Int J Elect Power Energy Syst 2013;53:209–18.
[4] Varricchio SL, Gomes Jr S, Diniz Rangel R. Three winding transformer s-domain model for modal analysis of electrical networks. Int J Elect Power Energy Syst 2011;33(3):420–9.
[5] Talaq J. Fault calculations using three terminal Thevenin's equivalent circuit. Int J Elect Power Energy Syst 2011;33(8):1462–9.
[6] Vlachogiannis JG. An accurate autotransformer model for load flow studies effect on the steady-state analysis of the Hellenic transmission system. Elect Power Syst Res 1999;50(2):147–53.
[7] Andrei RG, Rahman ME, Koeppel C, Arthaud JP. A novel autotransformer design improving power system operation. IEEE Trans Power Delivery 2002;17(2):523–7.
[8] Mork BA, Gonzalez F, Ishchenko D. Leakage inductance model for autotransformer transient simulation. In: International conference on power systems transients. Montreal, Canada, June 2005.
[9] Horton R, Dugan RC, Wallace K, Hallmark D. Improved autotransformer model for transient recovery voltage (TRV) Studies. IEEE Trans Power Delivery 2012;27(2):895–901.
[10] Delfino F, Procopio R, Rossi M. High-frequency EHV/HV autotransformer model identification from LEMP test data. IEEE Trans Power Delivery 2011;26(2):714–24.
[11] Kelemen T. Transformer tertiary and how to handle it. J Energy 1994;43:111–7.
[12] McMahon D. MATLAB demystified. McGraw-Hill Professional; 2007.
[13] Gajic Z, Holst S. Application of unit protection schemes for auto-transformers. In: 2nd International scientific and technical conference: actual trends in development of power system protection and automation. Moscow, September 2009.
[14] Gajic Z, Ivankovic I, Filipovic-Grcic B. Differential protection issues for combined autotransformer-phase shifting transformer. Int Conf Develop Power Syst Protect 2004;1:364–7.
[15] Dolenc A. Transformers 1 and 2, book, Faculty of electrical engineering and computing, 3rd ed. Zagreb; 1991.
[16] Sluis Lou van der. Transients in power systems. Chichester, England: John Wiley & Sons Ltd; 2001.